EPJ Web of Conferences **274**, 04001 (2022) https://doi.org/10.1051/epjconf/202227404001
XVth Quark Confinement and the Hadron Spectrum

The Overshadowed $\chi_{c1}(2p)$ Charmoniumlike Resonance

Roberto Bruschini[1,*]

[1]Unidad Teórica, Instituto de Física corpuscular (UV–CSIC), 46980 Paterna (Valencia), Spain

Abstract. A systematic analysis of $J^{PC} = 1^{++}$ charmoniumlike mesons with energies up to 4.0 GeV is carried out within the diabatic approach to QCD. The resulting spectrum contains only two bound states: the conventional $1p$ charmonium state and a $D^0\bar{D}^{*0}$ loosely bound state which may be naturally identified with $X(3872)$. The rest of the spectrum consists in a continuum of $D^0\bar{D}^{*0}$ and D^+D^{*-} scattering states, whose analysis indicates the presence of a resonance near 3.96 GeV that may be assigned to a mostly conventional $2p$ charmonium state. It is shown that this $\chi_{c1}(2p)$ resonance is likely overshadowed in its expected main decay channels, $D^0\bar{D}^{*0}$ and D^+D^{*-}, by the threshold enhancements due to the loosely bound $X(3872)$, which may justify its lack of detection to date. Alternative discovery channels are discussed.

1 Introduction

The discovery of the $X(3872)$ in 2003 [1] marked the beginning of a new era in hadron spectroscopy. In fact this state, despite showing a $c\bar{c}$ quark content from its observed decays to $J/\psi\,\pi\,\pi$, could not be put in correspondence with any quark model prediction, which before had been so successful for charmonium [2, 3]. Since then, the J^{PC} quantum numbers of $X(3872)$ have been determined to be 1^{++} (hence it has also been labeled as $\chi_{c1}(3872)$) and many other exotic heavy mesons have been discovered, see [4] and references therein.

The discovery of experimental states escaping the quark model spectrum has attracted an incredible amount of attention from the theoretical community in hadronic physics. But there is another equally surprising fact that has sometimes been overlooked. This is, some predicted quarkonium states have *not* been observed ever since, despite their masses being located in an easily accessible energy region.

Let us focus on one such quarkonium state that shares a close relation with the famous $X(3872)$: the $2p$ charmonium state with $J^{PC} = 1^{++}$, which we will refer to hereafter as $\chi_{c1}(2p)$. Its predicted mass is around 3.95 GeV, relatively far from any open-flavor meson-meson threshold which may distort its lineshape. It is also well-separated from other well-established charmoniumlike mesons with the same $J^{PC} = 1^{++}$ quantum numbers. It is expected to decay to $D\bar{D}^*$, but this does not necessarily mean that its width may be exceedingly large. Hence, there appears to be no *a priori* reason for which $\chi_{c1}(2p)$ should be considered an elusive particle.

As a matter of fact, however, there is no well-established candidate for $\chi_{c1}(2p)$ in the PDG listing of $c\bar{c}$ mesons as of today [4]. Instead, there are merely two unconfirmed candidates

*e-mail: roberto.bruschini@ific.uv.es

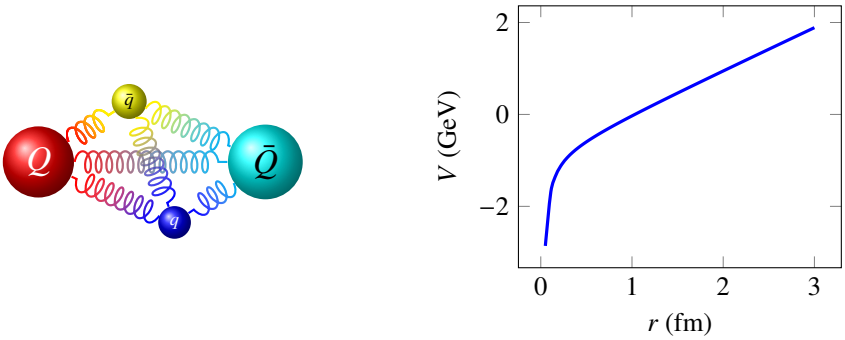

Figure 1. Left: pictorial representation of a quarkoniumlike meson as a heavy quark-antiquark pair ($Q\bar{Q}$) interacting with sea quarks (represented by a single light quark pair $q\bar{q}$) and gluons (represented by the colored coils connecting the quarks). Right: phenomenological funnel potential, representing the lowest static energy between a quark-antiquark pair interacting with gluons only (no sea quarks).

near the expected mass of $\chi_{c1}(2p)$: the $X(3940)$ peak in $D\bar{D}^*$, observed by Belle in 2007 [5], and a possible $X(3960)$ structure in $J/\psi\,\omega$, as noted by BESIII in 2019 [6].

In this talk, we attempt a phenomenological explanation of the elusive character of $\chi_{c1}(2p)$ and its relation to $X(3872)$. For this study, we work within the diabatic approach to QCD [7, 8]. This allows for a phenomenological treatment of quarkoniumlike mesons, underpinned by lattice QCD calculations of the static potentials between quark-antiquark and open-flavor meson-meson channels [9, 10].

The talk is organized as follows. In Section 2, we briefly recap the main features of the diabatic approach in QCD. In Secttion 3, we present the results of a phenomenological study of 1^{++} charmoniumlike mesons, including $X(3872)$ and $\chi_{c1}(2p)$, within the diabatic framework. Finally, in Section 4, we summarize our main conclusions.

2 Diabatic Approach

A quarkoniumlike meson system can be pictured as a heavy quark-antiquark pair interacting with gluons and light sea quarks, see left panel of Figure 1. This system shows a clear separation of its two characteristic energy scales, with the mass of the heavy quarks being much bigger than the QCD energy scale $\Lambda_{\rm QCD}$ governing the gluons and light fields. Because of this, when considering the time evolution of the light quarks and gluons, the heavy quarks move so slowly in comparison that they can be treated as being fixed into static positions. This is the core tenet of the Born-Oppenheimer approximation in QCD, see, for example, [11, 12] and references therein. The static energy levels of the gluons and light quark fields, which can be calculated in lattice QCD, are then identified in the Born-Oppenheimer approximation as effective potentials for the heavy degrees of freedom. Therefore, calculating the quarkoniumlike meson spectrum reduces to solving a multichannel Schrödinger equation with Born-Oppenheimer potentials, ideally taken from lattice QCD.

Ignoring the contributions from sea quarks, the lowest Born-Oppenheimer potential shows a short-range attractive Coulomb interaction and a linear confining behavior at large distances [13], bearing a close resemblance with the funnel potential used in quark models [2], see right panel of Figure 1. Hence, it may be said that the phenomenological quarkonium model found a theoretical foundation on lattice QCD, more than 20 years after its original formulation. Still, however, the quarkonium potential cannot account for $X(3872)$ nor for the

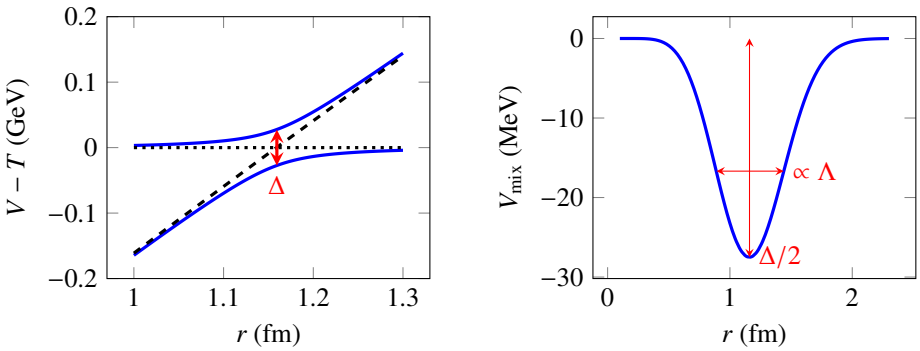

Figure 2. Left: phenomenological lowest and first excited Born-Oppenheimer potentials including sea quarks (solid lines), against the quarkonium potential (dashed line) and threshold mass (dotted line). Right: mixing potential between the quark-antiquark and open-flavor meson-meson channels.

elusive character of $\chi_{c1}(2p)$. This failure may be attributed, at least in part, to the fact that the quarkonium potential ignores the effects of open-flavor thresholds. This is necessarily so, in a Born-Oppenheimer perspective, as long as the calculation of the corresponding potential does not include dynamical light quarks.

As the steadfast technological advances allowed for more realistic lattice QCD simulations, calculations of Born-Oppenheimer potentials with dynamical light quarks paved the way for further progress [9, 10]. These calculations showed that the linear confining part of the lowest potential, instead of growing indefinitely, actually saturates at the mass T of the lowest open-flavor threshold with the right quantum numbers. This is somehow to be expected from the intuitive string breaking picture commonly used to explain color confinement. A less intuitive result is that there also appears an excited potential which shows the opposite behavior. In fact, the first excited potential starts at the threshold mass and then takes on a linear confining behavior after the lowest potential saturates. The two potentials come very close but fall short of crossing each other, being separated by an energy gap $\Delta > 0$. This phenomenon, known as avoided crossing or adiabatic surface mixing, is a clear indication that there is some mixing going on between the quark-antiquark and meson-meson configurations of the quarkoniumlike system. This situation is pictured in the left panel of Figure 2.

Whenever there is strong mixing between different channels in the Born-Oppenheimer approximation, the most convenient representation of the problem is given by the diabatic approach. In this representation, the multichannel Schrödinger equation describing a quarkoniumlike meson system made of one quark-antiquark and one meson-meson component may be intuitively written as[1]

$$\left[\begin{pmatrix} -\frac{\nabla^2}{2\mu_{Q\bar{Q}}} & 0 \\ 0 & -\frac{\nabla^2}{2\mu_{M\bar{M}}} \end{pmatrix} + \begin{pmatrix} V_{Q\bar{Q}}(\boldsymbol{r}) & V_{\mathrm{mix}}(\boldsymbol{r}) \\ V_{\mathrm{mix}}(\boldsymbol{r}) & T_{M\bar{M}} \end{pmatrix} - E\right] \begin{pmatrix} \psi_{Q\bar{Q}}(\boldsymbol{r}) \\ \psi_{M\bar{M}}(\boldsymbol{r}) \end{pmatrix} = 0 \tag{1}$$

where $\mu_{Q\bar{Q}}$ and $\mu_{M\bar{M}}$ are, respectively, the reduced masses of quark-antiquark and meson-meson, $\psi_{Q\bar{Q}}(r)$ and $\psi_{M\bar{M}}(r)$ their corresponding wave functions, $V_{Q\bar{Q}}(r)$ is the quarkonium potantial, $T_{M\bar{M}}$ the threshold mass, $V_{\mathrm{mix}}(r)$ the mixing potential between the two channels, and E the center-of-mass energy.

[1]The expression shown here is purely symbolic. The equation used in actual calculations is pretty cumbersome, even for two channels only. We refer the interested reader to [8] for details.

It is important to realize that the potential matrix in Equation (1), called diabatic potential matrix, treats on equal grounds the interactions within each channel as well as the coupling between quark-antiquark and meson-meson. Its eigenvalues are nothing but the lowest and first excited Born-Oppenheimer potentials with sea quarks.

The solutions to Equation (1) with $E < T$ represent bound states made of quark-antiquark and meson-meson components. These solutions may include quarkonium, molecular, and mixed states depending on the relative importance of the quark-antiquark and meson-meson total probabilities. In addition to eventual bound states, Equation (1) admits a continuum spectrum of solutions corresponding to open-flavor meson pairs with energy $E > T$, scattering off each other because of their common mixing with quark-antiquark at short distances. These continuum solutions may be used to calculate the meson-meson S-matrix, through which one can look for scattering resonances that may be of conventional (i.e., quarkonium) or unconventional nature.

3 $X(3872)$ and $\chi_{c1}(2p)$

The diabatic approach to QCD provides a framework in which to pursue a phenomenological analysis beyond quarkonium, taking into account the form of the Born-Oppenheimer potentials calculated on the lattice. Next, we study charmoniumlike mesons with $J^{PC} = 1^{++}$ and energy below 4.0 GeV within the diabatic framework [14]. The channels that we are going to consider are therefore $c\bar{c}$ (p-wave), $D^0\bar{D}^{*0}$ (s-wave and d-wave), and D^+D^{*-} (s-wave and d-wave).

In order to reproduce the successful description of the low-lying charmonium states by the quark model, for the radial form of the quarkonium potential $V_{Q\bar{Q}}(\boldsymbol{r})$ inside the potential matrix we take the funnel form plotted in the right panel of Figure 1,

$$V_{Q\bar{Q}}(r) = -\frac{\chi}{r} + \sigma r + 2m_c - \beta \tag{2}$$

with standard phenomenological values of the color Coulomb strength χ, string tension σ, and charm quark mass m_c [2]. Notice that we have decomposed the additive constant of the potential into a contribution from the quark-antiquark total mass and an additional constant β. We fix β so that the $1p$ charmonium mass calculated from this potential matches the experimental mass of $\chi_{c1}(1p)$. Notice also that the reduced quark-antiquark mass $\mu_{c\bar{c}}$ is simply $m_c/2$.

As for the charmed meson masses, m_{D^0}, m_{D^+}, $m_{D^{*0}}$, and $m_{D^{*+}}$, we take them from the PDG averages [4]. These determine the threshold masses $T_{M\bar{M}}$ and reduced masses $\mu_{M\bar{M}}$ for all meson-meson channels. So, for example, the $D^0\bar{D}^{*0}$ threshold is given by $m_{D^0} + m_{D^{*0}}$, and the corresponding reduced mass by $m_{D^0}m_{D^{*0}}/(m_{D^0} + m_{D^{*0}})$. We assume the threshold masses to be the main contributions to the static energies. Other meson-meson potentials, such as a mixing potential between $D^0\bar{D}^{*0}$ and D^+D^{*-}, are assumed to be negligible for our purposes.

Finally, the radial form of the quark-antiquark–meson-meson mixing potentials are parametrized with a Gaussian function,

$$V_{\text{mix}}(r) = -\frac{\Delta}{2}\exp\left[-\frac{1}{2}\left(\frac{V_{Q\bar{Q}}(r) - T_{M\bar{M}}}{\Lambda}\right)^2\right] \tag{3}$$

where Δ is the energy gap between two consecutive (effective) Born-Oppenheimer potentials at their avoided crossing and Λ is a parameter governing the width of the mixing region, see the right panel in Figure 2. We use unique values of Δ and Λ for both the $c\bar{c}$-$D^0\bar{D}^{*0}$ and $c\bar{c}$-D^+D^{*-} mixing potentials, consistently with approximate isospin symmetry.

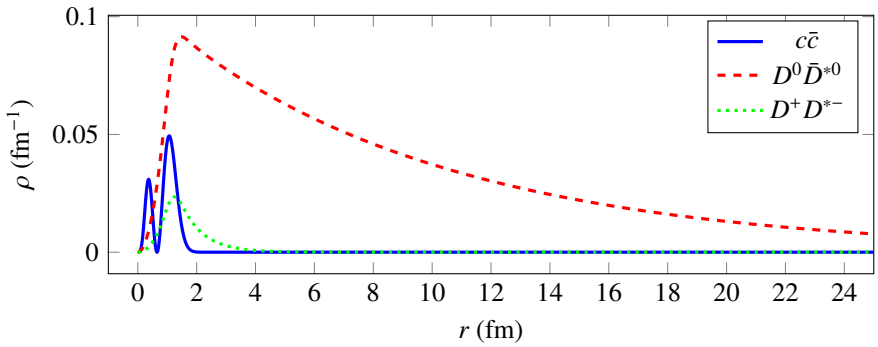

Figure 3. Radial probability densities for the diabatic $X(3872)$. The long tail of the molecular $D^0\bar{D}^{*0}$ component reaches up to $r \approx 70$ fm.

We fix the value of Λ, which is parametrization-dependent, requiring that the mixing between the quark-antiquark and meson-meson components takes place within a fraction of a fm from the avoided crossing between the Born-Oppenheimer potentials.

As for Δ, which is then the last remaining free parameter of the model, we fix its value by requiring that there appears an unconventional bound state close below the $D^0\bar{D}^{*0}$ threshold (specifically, at a mass of 3871.6 MeV), corresponding to $X(3872)$.

The calculated probability density of $X(3872)$ is made of comparable amounts of $c\bar{c}$, $D^0\bar{D}^{*0}$, and D^+D^{*-} components for $r \lesssim 1$ fm, whereas it is dominated by the weakly bound $D^0\bar{D}^{*0}$ component for $r > 2$ fm, see Figure 3. This very long $D^0\bar{D}^{*0}$ tail dominates the overall composition of $X(3872)$ with a 93% total probability (against a 4% of $c\bar{c}$ and 3% of D^+D^{*-}), and gives this state a huge root-mean-square radius of around 14 fm. Hence, in this diabatic picture the $X(3872)$ is represented as a loosely bound $D^0\bar{D}^{*0}$ state, where the binding is provided by a compact 2^3P_1 $c\bar{c}$ core.

After having fixated the parameters of the diabatic potential matrix using both phenomenology and hints from lattice QCD, we can calculate the open-charm meson-meson S-matrix for $J^{PC} = 1^{++}$. From it, we can calculate the elastic cross-sections plotted in Figure 4. Starting from zero at the mass of the $D^0\bar{D}^{*0}$ threshold, the $D^0\bar{D}^{*0}$ cross-section increases sharply, indicating the presence of the $X(3872)$ bound state close below threshold. Then, after a brief plateau, the threshold enhancement of the cross-section starts decreasing. First, there is a sudden decrease as the D^+D^{*-} threshold opens up, then the enhancement slowly fades as the energy increases further. On top of it, at around 3.96 GeV, there is a barely visible shoulder in the cross-section, which may be attributed to $\chi_{c1}(2p)$. A similar qualitative behavior is shown by the D^+D^{*-} cross-section, although with a smaller threshold enhancement.

To see the $\chi_{c1}(2p)$ more clearly, and understand the interplay between this resonance and the threshold enhancement due to $X(3872)$, we plot in Figure 5 the s- and d-wave Argand diagrams of the $D^0\bar{D}^{*0}$ elastic scattering.[2] These diagrams show the path followed by the partial-wave scattering amplitudes on the complex plane, which have well-understood behaviors for shallow bound states and resonances:

a) if there is a shallow bound state with angular momentum l, the low-energy l-wave scattering amplitude moves quickly clockwise along the unitary circle;

[2]The Argand diagrams for D^+D^{*-} follow a similar pattern.

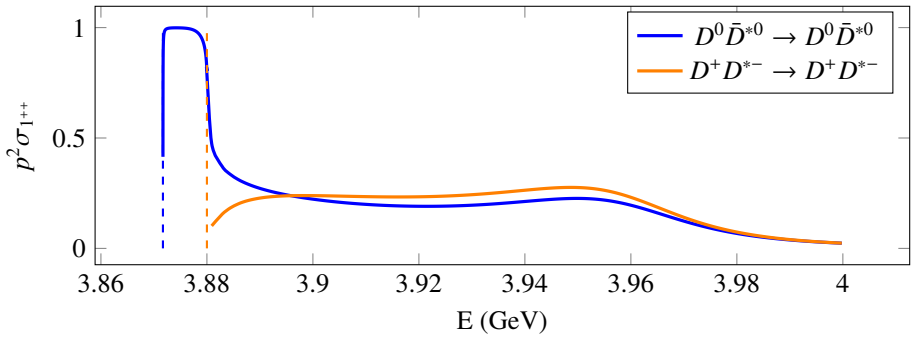

Figure 4. Calculated cross-sections for $J^{PC} = 1^{++}$, scaled by the relative momentum squared.

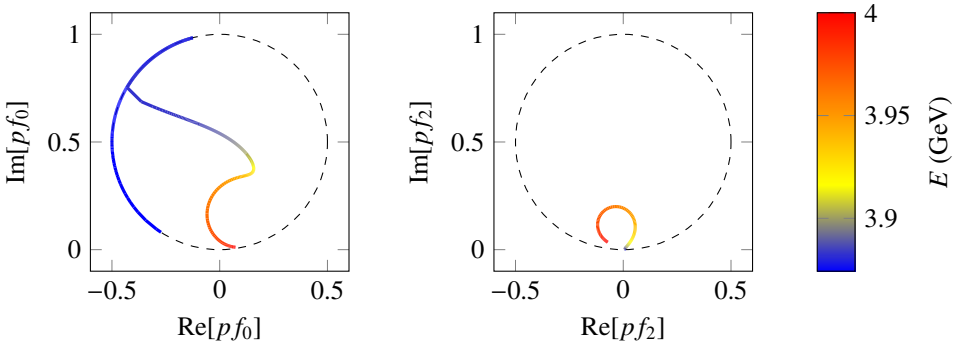

Figure 5. Calculated Argand diagrams for elastic $D^0\bar{D}^{*0}$ scattering in s-wave (left) and d-wave (right). The unitary circle is drawn with a dashed line.

b) if there is a resonance, all scattering amplitudes coupling to it perform a 2π counterclockwise rotation for energies close to the resonance mass.

Comparing the known behaviors a) and b) with the Argand diagrams in Figure 5, a clear physical picture for $\chi_{c1}(2p)$ emerges. The s-wave diagram on the left panel shows behavior a) at small energies, consistently with the presence of the diabatic $X(3872)$, which is predominantly a s-wave $D^0\bar{D}^{*0}$ molecule. Because the d-wave component in the calculated $X(3872)$ is largely suppressed, this same behavior is absent from the d-wave diagram on the right panel. Then, at energies close to 3.96 GeV, the d-wave Argand diagrams show clearly the pattern b), indicating the presence of the $\chi_{c1}(2p)$ resonance. This resonant behavior, however, is not as easily readable from the s-wave Argand diagram, because of the coherent sum between the waning threshold enhancement a) and the resonant behavior b).

Therefore, we can conclude that the threshold enhancements produced by $X(3872)$ overshadow the $\chi_{c1}(2p)$ resonance in the open-charm meson-meson channels. Since these OZI-allowed decays are expected to be the main decay channels of $\chi_{c1}(2p)$, this overshadowing may be the principal reason behind its elusiveness.

However, it is possible that this overshadowing does not occur for other decay channels, making them the preferred way for detection. In fact, the d-wave $D^0\bar{D}^{*0}$ Argand diagram in Figure 5 shows very clearly the presence of $\chi_{c1}(2p)$ despite the $X(3872)$. This is because,

as mentioned before, the d-wave $D^0\bar{D}^{*0}$ component is negligible in $X(3872)$, hence the enhancement is not so severe in that channel. While it is clearly unfeasible to resolve d-wave $D^0\bar{D}^{*0}$ from data, this fact makes us hopeful that other decay channels, which do not appear as bound components in $X(3872)$, might provide a clear signal for $\chi_{c1}(2p)$.

4 Summary

We have analyzed charmoniumlike mesons with $J^{PC} = 1^{++}$ and energy below 4.0 GeV using the diabatic approach in QCD. This includes the conventional $\chi_{c1}(1p)$ and unconventional $X(3872)$ bound states, plus an analysis of $D^0\bar{D}^{*0}$ and D^+D^{*-} elastic scattering for center-of-mass energies below 4.0 GeV.

First, we have summarized the main features of the diabatic approach. We have shown that this formalism provides the most convenient scheme for constructing a potential model which includes the main features of the Born-Oppenheimer potentials calculated in lattice QCD. Specifically, we have seen that the avoided crossing observed on the lattice can be understood in terms of a mixing potential between the quark-antiquark and open-flavor meson-meson channels. Below threshold, the mixing can generate new unconventional bound states with molecular components. Above threshold, it mediates meson-meson scattering through short-range quark-antiquark interactions, e.g., $D^0\bar{D}^{*0} \to c\bar{c} \to D^0\bar{D}^{*0}$.

We have shown that the $X(3872)$ can be described in the diabatic framework as a mostly molecular $D^0\bar{D}^{*0}$ state. We have further shown that, because of its composition and closeness to the open-charm thresholds, the $X(3872)$ produces important enhancements in the $D^0\bar{D}^{*0}$ and D^+D^{*-} cross-sections at low energy.[3] These enhancements may overshadow the conventional $\chi_{c1}(2p)$ resonance, whose mass is predicted near 3.96 GeV, such that it may not be easily visible in its only OZI-allowed channels. We argued that other decays, provided that their products do not overlap with the molecular components of $X(3872)$, may constitute more favorable discovery channels.

This work has been supported by Ministerio de Ciencia e Innovación and Agencia Estatal de Investigación of Spain MCIN/AEI/10.13039/501100011033 and European Regional Development Fund Grant No. PID2019-105439 GB-C21, by EU Horizon 2020 Grant No. 824093 (STRONG-2020), by Conselleria de Innovación, Universidades, Ciencia y Sociedad Digital, Generalitat Valenciana GVA PROMETEO/2021/083, and by a Formación de Personal Investigador fellowship from Ministerio de Ciencia, Innovación y Universidades of Spain under Grant No. BES-2017-079860.

References

[1] S.K. Choi et al. (Belle Collaboration), Phys. Rev. Lett. **91**, 262001 (2003)
[2] E. Eichten, K. Gottfried, T. Kinoshita, K.D. Lane, T.M. Yan, Phys. Rev. D **17**, 3090 (1978)
[3] S. Godfrey, N. Isgur, Phys. Rev. D **32**, 189 (1985)
[4] R.L. Workman (Particle Data Group), Prog. Theor. Exp. Phys. **2022**, 083C01 (2022)
[5] K. Abe et al. (Belle), Phys. Rev. Lett. **98**, 082001 (2007)
[6] M. Ablikim et al. (BESIII Collaboration), Phys. Rev. Lett. **122**, 232002 (2019)
[7] R. Bruschini, P. González, Phys. Rev. D **102**, 074002 (2020)
[8] R. Bruschini, P. González, Phys. Rev. D **104**, 074025 (2021)
[9] G.S. Bali, H. Neff, T. Düssel, T. Lippert, K. Schilling (SESAM Collaboration), Phys. Rev. D **71**, 114513 (2005)

[3] This holds true even if $X(3872)$ were described as a slightly virtual state instead of a shallow bound state.

[10] J. Bulava, B. Hörz, F. Knechtli, V. Koch, G. Moir, C. Morningstar, M. Peardon, Phys. Lett. B **793**, 493 (2019)
[11] K.J. Juge, J. Kuti, C.J. Morningstar, Phys. Rev. Lett. **82**, 4400 (1999)
[12] E. Braaten, C. Langmack, D.H. Smith, Phys. Rev. D **90**, 014044 (2014)
[13] G.S. Bali, Phys. Rep. **343**, 1 (2001)
[14] R. Bruschini, P. González, submitted for publication (2022), arXiv:2207.02740